Korean J. Chem. Eng., 33(11), 3169-3174 (2016)
DOI: 10.1007/s11814-016-0196-1

pISSN: 0256-1115
eISSN: 1975-7220

Low temperature synthesis of *Manganese tungstate* nanoflowers with antibacterial potential: Future material for water purification

Musarat Amina*, Touseef Amna,****,†, Mallick Shamshi Hassan***,****, Nawal Musayeib Al Musayeib*, Salem Slayyem Salem Al-Deyab*****, and Myung-Seob Khil****,†**

*Department of Pharmacognosy, Pharmacy College, King Saud University, Riyadh11451, Kingdom of Saudi Arabia
**Department of Biology, Faculty of Science, Albaha University, Albaha 1988, Kingdom of Saudi Arabia
***Department of Chemistry, Faculty of Science, Albaha University, Albaha 1988, Kingdom of Saudi Arabia
****Department of Organic materials and Fiber Engineering, Chonbuk National University, Jeonju 54896, Korea
*****Petrochemical Research Chair, Department of Chemistry, College of Science,
King Saud University, Riyadh 11451, Saudi Arabia
(*Received 9 February 2016 • accepted 2 July 2016*)

Abstract−Pure water is the fundamental requisite for human life. The water has been recycled naturally but not in an adequate amount for consumption. Nanotechnology with extraordinary applications provides competent ways for the decontamination of contaminated water. In the present study $MnWO_4$ nanoflowers endorsed with inherent antibacterial activity were successfully synthesized by facile hydrothermal approach. XRD, SEM, EDX spectroscopy and UV-DRS were used to characterize the as-synthesized nanoflowers. Gram negative *Escherichia coli* ATCC 52922 bacterium was used as model organism to test antibacterial activity of as-synthesized $MnWO_4$ nanoflowers. This study was conducted to optimize minimum concentration of $MnWO_4$ nanoflowers and maximum contact time required to achieve complete inactivation of bacteria present in contaminated water. Minimum inhibitory concentration (MIC) of $MnWO_4$ nanoflowers was found to be 10 μg/ml. The assessment and interpretation of bacterial viability was done using dual fluorescent staining. The synthesized 3D-nanoflowers were found as potent bactericides. Thus, $MnWO_4$ nanoflowers emerged to be very good future material for disinfection of biological pollutants present in the contaminated water reservoirs and as an anti-biofouling agent.

Keywords: Water, Antibacterial, Hydrothermal, $MnWO_4$, *Escherichia coli*

INTRODUCTION

It has been recognized that the waterborne diseases are the second leading cause of death in children below the age of five years worldwide. The textile industry is an important water consumer and thus produces highly colored and complex wastewater. Also, enormous quantities of effluents from industries are discharged in water. The industrial wastewater treatment is therefore a very important issue. Various approaches have been adapted in past for the treatment of waste water [1-6]. For instance, Choi et al. treated the dye waste water with zero-valent iron [2]. Singha et al. investigated packed column for removal of chromium from effluent wastewater [3]. In another report conductive activated charcoal plate has been utilized for the treatment of industrial wastewater [4]. It is expected that 10% of global diseases can be controlled by improving the water supply, sanitation, hygiene and proper management of water resources [5,6]. Annually more than 3.4 million people (especially children) die from waterborne infections. This is the approximation data of the World Health Organization (WHO). WHO characterize safe drinking water as water which fulfills national standards with respect to microbial, physical and chemical properties [7]. Moreover, the greatest threat posed to drinking water resources arises from bacterial contamination, as they cause diseases which could be life-threatening upon exposure. WHO urges total coliform count of zero in 100 ml sample [8] of water that is wished for drinking purposes. In this regard many traditional methods, both chemical (chlorine, ozone, iodine) and physical (ultraviolet radiation) [9,10] have been applied to inactivate bacteria in water supplies. Nevertheless, these methods can effectively eliminate/or reduce pathogenic bacteria to the desired levels. However, recently research has revealed that such methods can lead to formation of harmful disinfection byproducts [11,12].

Keeping in consideration the resistance of pathogenic bacteria in water, the search for new disinfection agents has become a vital subject. In the past two decades, advances in nanotechnology have extended the possibilities for development of high performance nanomaterials, targeted at solving the current problems related to unhygienic quality of water. Kalyani et al. adopted low temperature approach for the synthesis of various transition metal oxides and also investigated their antibacterial activity against multidrug resistance bacterial pathogens [13]. Very recently, in another report bioactive glass and poly(vinyl alcohol) composites prepared by melting and sol-gel techniques have been utilized as antibacterial materials for disinfection [14]. In general, the nanoscale materials can

†To whom correspondence should be addressed.
E-mail: touseefamna@gmail.com, mskhil@jbnu.ac.kr

be categorized as metal/oxide nanomaterials, carbonaceous nanomaterials, zeolites and dendrimers which are being more often evaluated for use as functional materials for purification of water. These materials possess a broad range of physico-chemical properties that make them attractive for use as separation and reactive media for water treatment [15,16]. Herein, we report the facile preparation of semiconductor manganese tungstate nanoflowers and the synthesized nanoflowers were for the first time applied as antibacterial agents for purification of waste water. Manganese tungstate ($MnWO_4$) has a wolframite type monocline structure, where the manganese and tungsten atoms are surrounded by six oxygen which form distorted octahedrons [MnO_6]/[WO_6] clusters [17]. $MnWO_4$ crystals have been extensively explored because nanocrystals present a great number of properties, such as magnetic [18,19], multiferroic [20,21], photocatalysis [22], photoluminescence [23,24] and as a humidity sensor [25]. Several synthesis methods (aqueous and solvothermal reactions) have been employed in the preparation of $MnWO_4$ crystals. However, these methods reflect some disadvantages such as long processing time and use of high temperature [26,27]. In this article, we describe a simple hydrothermal approach, without the use of any surfactant or/template for synthesis of $MnWO_4$ nanoflowers. The obtained nanoflowers were therefore expected to demonstrate effective antibacterial activity against *Escherichia coli* (*E. coli*) bacteria. The *E. coli* serves as representative Gram-negative bacterium which is most frequently present in contaminated water. Nevertheless, there is no report on the antibacterial properties of $MnWO_4$ nanoflowers.

MATERIALS AND METHODS

1. Material Synthesis

$MnWO_4$ nanoflowers were prepared by hydrothermal method using $Na_2WO_4{\cdot}2H_2O$ and $Mn(NO_3)_2$ (Samchun Chemical Ltd., 99% and 98%) as precursors. In brief, 1.65 g of $Na_2WO_4{\cdot}2H_2O$ and 1.44 g of $Mn(NO_3)_2$ were separately dissolved in 50 ml of deionized water. Both the aqueous solutions were mixed slowly and the pH of resulting solution was adjusted (~9.0) by adding liquid ammonia (Samchun Chemical Ltd., 28-30%). The solutions were subsequently transferred into a Teflon-lined stainless steel autoclave (120 ml capacity), sealed and maintained at 180 °C for 24 h. The reaction mixture was cooled at room temperature. The obtained precipitate was washed with distilled water, separated by filtration and the filtrate was dried at 80 °C overnight in an oven. $MnWO_4$ nanoflowers were obtained as final product.

2. Characterization

X-ray diffraction (XRD) patterns of the samples were recorded on a Rigaku/Max-3A X-ray diffractometer. Field emission scanning electron microscope (FESEM, JEOL JSM6700) was used to observe the morphology of pure samples and the diameters of individual nanorods was measured using ImageJ software. Energy dispersive X-ray (EDX) spectroscopy connected with the scanning electron microscope (SEM) was used to analyze the composition of samples. The light absorbance of the samples was measured using UV-Vis diffused reflectance spectrum (UV-DRS, 525 Shimadzu).

3. Antibacterial Activity of $MnWO_4$ Nanoflowers

E. coli ATCC 52922 purchased from American Type Culture Collection (ATCC) was used as a model organism in the present study to evaluate the antimicrobial activity of $MnWO_4$ nanoflowers [28]. The bacterial strain was first cultured on agar plates. After growth, the fresh colonies were inoculated into 100 ml of broth (Tryptone soya broth). Growth was monitored at every 4 h by UV-Vis spectrophotometer till optical density reached 0.1 at 600 nm (OD of 0.1 corresponded to a concentration of 10^8 CFU/ml of medium). To check the minimum inhibitory concentration (MIC) of as-synthesized $MnWO_4$ nanoflowers, 1 ml of fully grown culture was inoculated to 100 ml of freshly prepared culture broth supplemented with different concentrations (5, 10, 20 and 25 μg/ml) of $MnWO_4$. The bacterial cultures were grown under dark conditions also and treated with $MnWO_4$ nanoflower samples as aforementioned. All the flasks were incubated at 37 °C in a rotary shaker at 150 rpm. Bacterial concentration was measured by optical density (OD) with absorbance at 600 nm by UV-spectrophotometer at an interval of 4 h for 16 h. The *E. coli* culture without the addition of $MnWO_4$ nanoflowers was treated as control sample.

4. Estimation of Bacterial Toxicity

To get number of live and dead bacteria at specific time interval, fluorescence staining was performed using live/dead BacLight bacterial viability kit. The *E. coli* bacteria was stained with fluorescent dyes strictly following the manufacturer's instructions and observed with confocal laser scanning microscopy (CLSM) as described elsewhere [29].

5. Statistical Analysis

In this study the statistical analysis of the experimental data was performed by ANOVA with the help of SPSS, 19.0 software packages, with multiple comparisons using least significant difference.

RESULTS AND DISCUSSION

At present, most of the natural water reservoirs are significantly contaminated with pathogenic bacteria. A large number of diseases which are widespread in developing countries are through consumption of contaminated water [30]. Nanomaterials with interesting applications have unwrapped the ways for improvement of methods for the treatment of wastes. These methods generally include decontamination of the contaminants from water due to reactive surface of smart materials, induce coating on pollutant to restrain the toxicity of compounds and kill the pathogens. Hence, there is noteworthy application of such type of antibacterial nanomaterials in water purification system developments. In the present study, well-designed, high aspect ratio, monodispersed 3D nanoflower clusters of $MnWO_4$ were synthesized by facile hydrothermal approach. The reaction was carried out at different temperatures (120, 140 °C) with varying time (such as 12 and 18 h, respectively). But no nanoflowers have been obtained. The reaction parameters such as temperature, duration and suitable pH feasible to get consistent flower like morphology were found to be 180 °C, 24 h and 9, respectively. The morphological characteristics depicted the chic flower structure of $MnWO_4$. One can predict the possible growth mechanism for the formation of $MnWO_4$ nanoflowers. When the manganese nitrate is mixed with sodium tungstate in basic medium, Mn^{2+} and WO_4^{2-} ions were formed. The partial positive charge of water molecule attracts the Mn^{2+} and the

partial negative charge attract the WO_4^{2-} ions, together they formed the nuclei which aggregate to form the $MnWO_4$ nanocrystals. With increasing reaction time, these nuclei were assembled and formed rods like structures. Finally they self-assembled and formed flower like morphology [31].

The XRD spectrum of the perfect $MnWO_4$ nanoflowers is shown in Fig. 1. The XRD pattern in the figure could be perfectly indexed as monoclinic structure for $MnWO_4$ (JCPDS 74-1497), respectively. The diffraction peaks of the $MnWO_4$ were sharp and intense, indicating the highly crystalline character of the nanoflowers. No impurity peak was found in $MnWO_4$, which suggests that the sample has only one-phase. Fig. 2 shows the SEM micrographs of the synthesized $MnWO_4$ nanoflowers at different magnifications. Fig. 2(a) and (b) demonstrate SEM images of $MnWO_4$ uniform clusters of nanoflowers. High magnification images clearly depict that flower shaped structures are composed of numerous individual $MnWO_4$ nanorods. The typical diameters of these individual nanorods were in the range of 600-700 nm with the length of 2-3 μm. From the morphology it is given to understand that all the nanorods apparently originated from a single center, which was eventually arranged in a spherical shape exhibiting typical flower like morphology. Fig. 3 shows energy-dispersive X-ray spectroscopy (EDX) spectrum of the $MnWO_4$ nanoflowers. The peaks corresponding to Mn, W and O are clearly identified. Fig. 4 depicts the UV-vis diffuse reflectance (DR) spectra of the $MnWO_4$ nanoflowers. UV-Vis spectra revealed that $MnWO_4$ nanoflowers had strong light absorption properties both in ultraviolet and visible region. In Fig. 4, absorption edges of $MnWO_4$ nanoflowers appeared at 707 nm, respectively, which corresponds to the band gap of $MnWO_4$ (1.75 eV).

WHO characterized safe drinking water as water whose microbial load is theoretically nil. Proper sanitation, hygiene and ade-

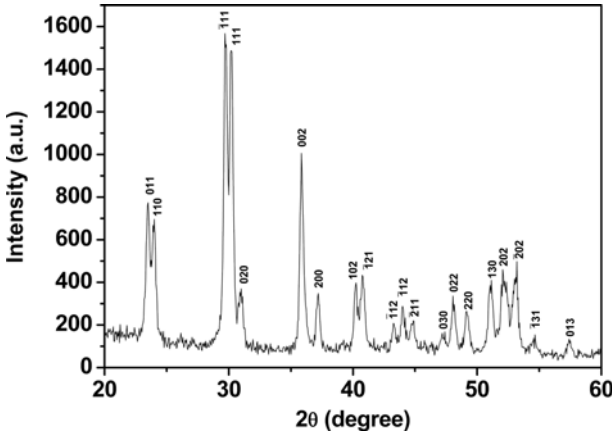

Fig. 1. XRD patterns of $MnWO_4$ nanoflowers.

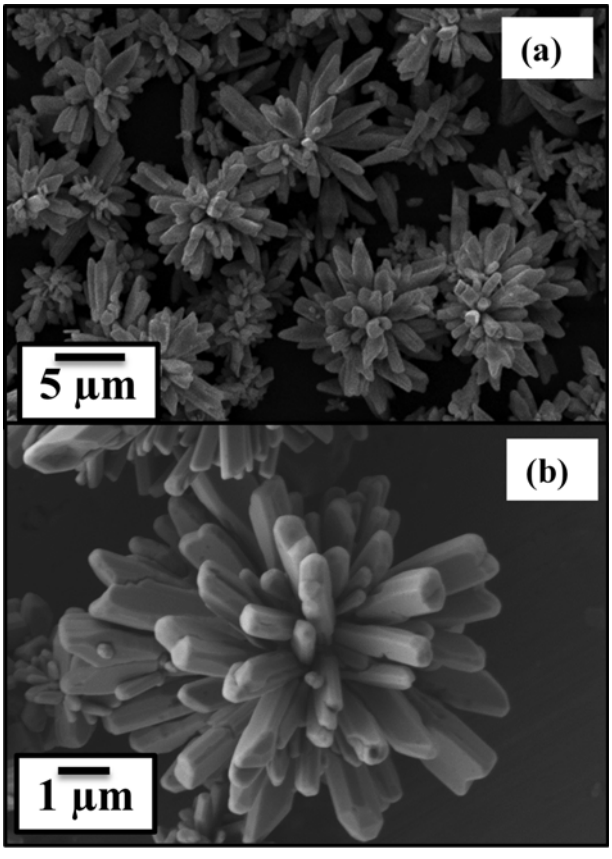

Fig. 2. SEM images of (a); (b) $MnWO_4$ nanoflowers at different magnifications.

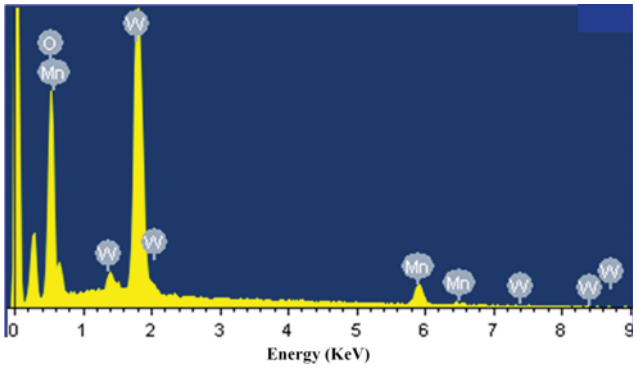

Fig. 3. EDX spectrum of $MnWO_4$ nanoflowers.

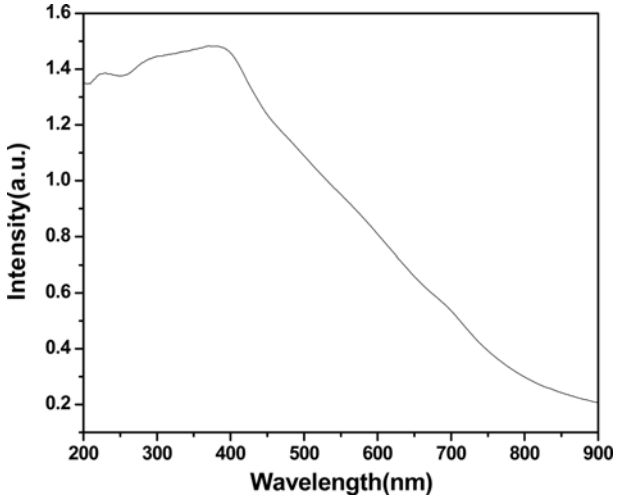

Fig. 4. UV-vis DRS spectrum of $MnWO_4$ nanoflowers.

quate management of water resources can help improving water supply. Also, it is expected that 10% of global diseases can be prevented by improving water quality. In this direction, currently nanoscience has provided the greater opportunities for the safe purification methods of water. The Gram negative bacterium *E. coli* has been selected as model organism for the investigation of antibacterial potential of $MnWO_4$ nanoflowers. The growth rate was estimated on the basis of OD taken at regular time intervals. The optimum growth was obtained during the log phase which extended from 4 to 12 h in the present study. After that the doubling rate decreased and a stationary phase was observed in case of control *E. coli* cells. To examine the antibacterial effect, five different concentrations as aforementioned have been used. The observed minimum inhibitory concentration of $MnWO_4$ for antibacterial activity was found to be 10 μg/ml (Fig. 5(a)). With the increase in concentration of $MnWO_4$, inhibition has also been increased. At the highest concentration of 25 μg/ml, prominent inhibition was observed (Fig. 5(a)). Interestingly, the $MnWO_4$ 3D nanoflowers depicted the antibacterial effect on *E. coli* cells under dark conditions also. However, the antibacterial efficiency was found less in case of dark with the same concentrations (Fig. 5(a)). Furthermore, the highest concentration (25 μg/ml) was found to be most detrimental for *E. coli* cells. Our results indicated that inhibitory efficacy depends upon concentration and contact time. To get insight into the cell death the exposed bacterial cells were stained with fluorescent dyes. These dyes are nucleic acid specific. The kit consists of two stains, propidium iodide (PI) and SYTO9. Fig. 5(b) and (c) demonstrates the representative CLSM images of *E. coli* before and after staining. Green fluorescing SYTO9 is able to enter all cells and is used for assessing total cell counts (Fig. 5(b)), whereas red fluorescing PI enters only cells with damaged cytoplasmic membranes (Fig. 5(c)). Live cells have intact membranes and are impermeable to dyes such as PI. From the CLSM images, it is quite evident that only dead *E. coli* cells were found in high concentration (25 μg/ml) of $MnWO_4$. Once again it was confirmed that the toxicity is concentration and contact time dependent (Fig. 5(a)).

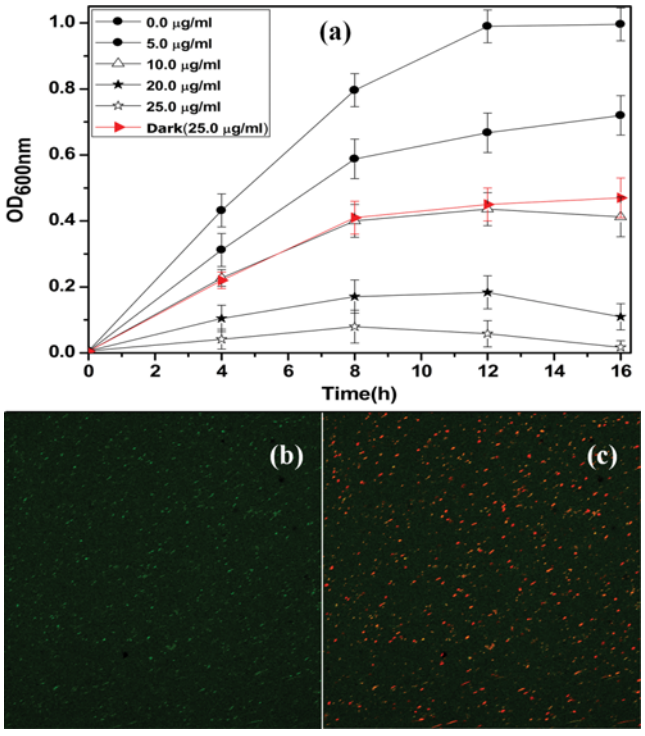

Fig. 5. Growth kinetics of *E. coli* cells (a) exposed to different concentrations of $MnWO_4$ nanoflowers. The experiments were conducted at least in triplicate and a difference was considered to be statistically significant at a value P<0.05. The statistical computations were run on SPSS-19.0, statistical software. At all the selected concentrations (5, 10, 20, 25 μg/ml (light), 25 μg/ml (dark), the OD values are significant at a value p<0.05. At the culture time of 12, 16 h, the OD value for all the above mentioned concentrations are significant at a value p<0.05 (b) Representative CLSM images of *E. coli* control cells (c) exposed to $MnWO_4$ nanoflowers (25 μg/ml).

Understanding the mechanism of toxicity of nanomaterials to biological systems is critical feature in the biomedical sciences. The major cause of bacterial toxicity of nanosized materials can be explained on the basis of membrane and oxidative stress as previously explained in the available literature [28,32]. The membrane stress is due to the direct contact which occurred between the $MnWO_4$ and chosen bacteria which have lead to disruption of bacterial cell wall and finally cell death [28,33]. Earlier study also reported the antibacterial effect of Mn_2O_3 nanowires and the authors have given the hypothesis for possible mechanism. In their study they indicated the interaction and accumulation of Mn^{3+} ions in bacterial cells walls after the dispersion of Mn_2O_3 nanowires in liquid medium [34]. In the present study, there is possibility of photocatalytic effect in which there is generation of reactive radicals upon irradiation under visible light. $MnWO_4$ 3D nanoflowers continuously interact with bacterial cells, and thus they exhibit an excellent toxicity against the selected *E. coli*. The OD as a function of time is shown in Fig. 5(a). The detrimental effect on bacteria of $MnWO_4$ 3D nanoflowers has been further elucidated via CLSM images. Fig. 5(b) and (c), show *E. coli* and *E. coli* with $MnWO_4$ 3D nanoflowers at high concentration. The plausible acting method can be explained like this. In case of *E. coli,* it is assumed that the $MnWO_4$ 3D nanoflowers have attached at outer membrane of bacterial cell, which has further led to cell breakage, finally resulting in cell lysis. However, the $MnWO_4$ 3D nanoflowers attached to the outer wall of cell in the beginning, and further, they perforated internal envelope of cell resulting in the damage of cell membrane, the disorganized intracellular contents seeped out, resulting in complete damage of bacterial cell. Gram-negative bacteria including *E. coli* exhibit only a thin peptidoglycan layer between the cytoplasmic membrane and outer membrane. We believe that when $MnWO_4$ 3D nanoflowers were dispersed in medium, the Mn^{2+} atoms present in $MnWO_4$ 3D nanoflowers interacted with the bacterial cells and adhered to the bacterial cell walls. The overall charge on the bacterial cell surface at biological pH is negative and is due to excess number of carboxylic and other groups that upon dissociation make cell surface negative [35]. The bacteria and the Mn^{2+} atoms in the $MnWO_4$ 3D nanoflowers have opposite charges, and these electrostatic forces may be the reason for their adhesion and bioactivity. Thus both free radicals and electrostatic forces are the most likely the reason for the detrimental effect of $MnWO_4$ 3D

nanoflowers in the present study. Thus, we can conclude from the obtained results that the prepared $MnWO_4$ are promising candidate to be used as an excellent antibacterial agent for purification of wastewaters.

CONCLUSION

Novel $MnWO_4$ nanoflowers with uniform sized nanorods were successfully synthesized using the easy hydrothermal method. The morphological characteristics depicted the chic flower structure of $MnWO_4$. The investigation of antibacterial ability indicated that the $MnWO_4$ nanoflowers possess potential antibacterial activity against the common water contaminant *E. coli*. Interestingly, the $MnWO_4$ nanoflowers have shown activity under dark conditions also. However, the detrimental effect of 3D $MnWO_4$ nanoflowers on bacteria was comparatively less significant under dark conditions. Thus, our results clearly indicate that the investigated nanoflowers are potential antibacterial materials that may be used to combat waterborne bacteria. Conclusively, clean water is basic requirement of life and our study proposes a new idea of using $MnWO_4$ for cleaning of wastewater (Fig. 6). Furthermore, the 3D $MnWO_4$ nanoflowers possess wide-range effect as the activity was observed both under light and dark. However, complete study is needed to investigate the other physicochemical properties of $MnWO_4$ nanoflowers before this material can be practically utilized for purification of contaminated water especially for drinking purposes.

ACKNOWLEDGEMENTS

This work was supported by the Industrial Strategic Technology Development Program, 10041994, funded by Ministry of Knowledge Economy (MKE, Korea). The authors also extend their appreciation to the vice Deanship of Scientific Research Chair at King Saud University for the help in research work.

SYMBOLS

μg	: microgram
ml	: milliliter
°C	: centigrade
μm	: micrometer
θ	: theta
°	: angle

Abbreviations

ATCC	: American type culture collection
OD	: optical density
PI	: propidium iodide
XRD	: X-ray diffraction

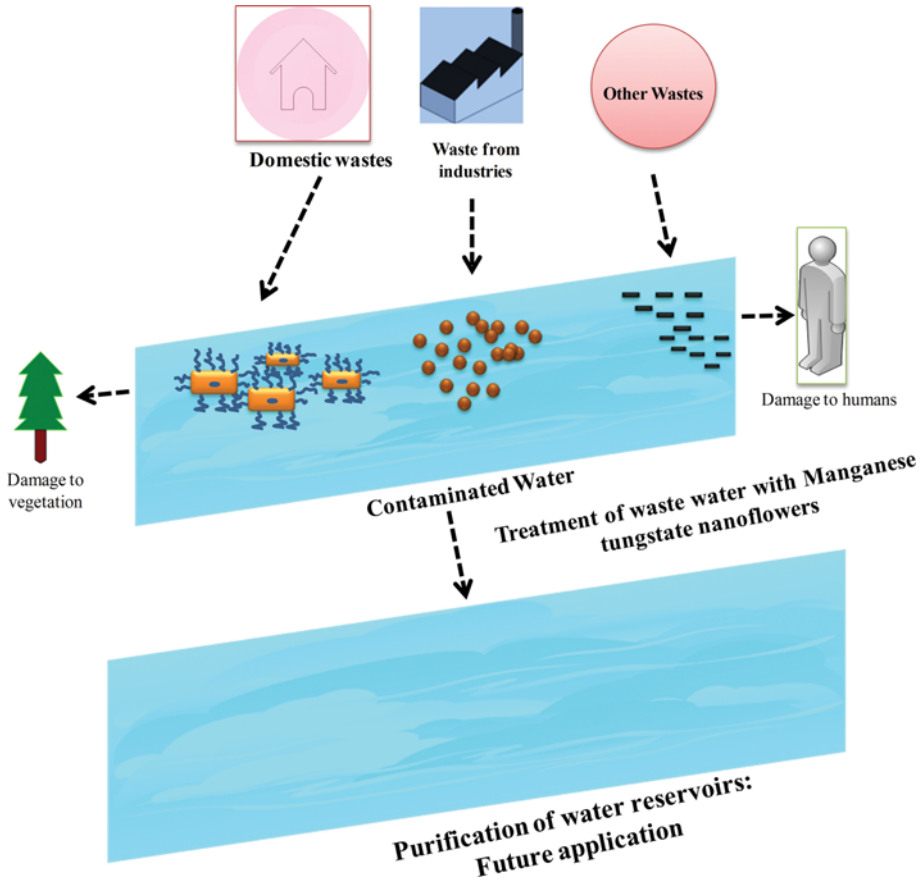

Fig. 6. Schematic diagram illustrating the use of as-synthesized $MnWO_4$ for cleaning of wastewater reservoirs.

FE-SEM : field emission scanning electron microscope
EDX : energy dispersive X-ray
UV-DRS : ultra violet diffused reflectance spectrum

REFERENCES

1. S. H. Khorzughy, T. Eslamkish, F. D. Ardejani and M. R. Heydartaemeh, *Korean J. Chem. Eng.*, **32**, 88 (2015).
2. Y. Choi, B. Park and D. K. Cha, *Korean J. Chem. Eng.*, **32**, 1812 (2015).
3. S. Singha and U. Sarkar, *Korean J. Chem. Eng.*, **32**, 20 (2015).
4. B. A. Feiz and S. Aber, *Korean J. Chem. Eng.*, **32**, 2014 (2015).
5. A. Prüss-Üstün, R. Bos, F. Gore and J. Bartram, World Health Organization (2008).
6. W. Kim, B. G. Ryu, S. Kim, S. W. Heo, D. H. Kim, J. Kim, H. Jo, J. H. Kwon and J. W. Yang, *Korean J. Chem. Eng.*, **31**, 381 (2014).
7. S. Pedley and K. Pond, World Health Organization (2003).
8. W. H. Organization, World Health Organization (2004).
9. G. A. Boorman, *Environ. Health Perspect.*, **107**, 207 (1999).
10. Y.-T. Woo, D. Lai, J. L. McLain, M. K. Manibusan and V. Dellarco, *Environ. Health Perspect.,* **110**, 75 (2002).
11. S. D. Richardson, *TrAC Trends Anal. Chem.*, **22**, 666 (2003).
12. A. Kamari, W. W. Ngah, M. Chong and M. Cheah, *Desalination*, **249**, 1180 (2009).
13. R. L. Kalyani, J. Venkatraju, P. Kollu, N. H. Rao and S. V. N. Pammi, *Korean J. Chem. Eng.*, **32**, 911 (2015).
14. S. Boulila, H. Oudadesse, H. Elfeki, R. Kallel, B. Lefeuvre, M. Mabrouk, S. Tounsi, D. Mhalla, A. Mostafa and K. Chaabouni, *Korean J. Chem. Eng.*, **33**, 1659 (2016).
15. N. Savage and M. S. Diallo, *J. Nanopart. Res.*, **7**, 331 (2005).
16. D. K. Tiwari, J. Behari and P. Sen, *World Appl. Sci. J.*, **3**, 417 (2008).
17. V. Felea, P. Lemmens, S. Yasin, S. Zherlitsyn, K. Choi, C. Lin and C. Payen, *J Phys.: Cond. Matt.*, **23**, 216001 (2011).
18. H. Ehrenberg, H. Weitzel, R. Theissmann, H. Fuess, L. Rodriguez-Martinez and S. Welzel, *Physica B: Cond. Matt.*, **276**, 644 (2000).
19. G. Lautenschläger, H. Weitzel, T. Vogt, R. Hock, A. Böhm, M. Bonnet and H. Fuess, *Phys. Rev. B*, **48**, 6087 (1993).
20. L. H. Hoang, N. Hien, W. Choi, Y. Lee, K. Taniguchi, T. Arima, S. Yoon, X. Chen and I. S. Yang, *J. Raman Spectrosc.*, **41**, 1005 (2010).
21. H. Zhou, Y. Yiu, M. Aronson and S. S. Wong, *J. Solid State Chem.*, **181**, 1539 (2008).
22. H. He, J. Huang, L. Cao and J. Wu, *Desalination*, **252**, 66 (2010).
23. S. Thongtem, S. Wannapop, A. Phuruangrat and T. Thongtem, *Mater. Lett.*, **63**, 833 (2009).
24. Y. Xing, S. Song, J. Feng, Y. Lei, M. Li and H. Zhang, *Solid State Sci.*, **10**, 1299 (2008).
25. W. Qu and J.-U. Meyer, *Sensors Actuat. B: Chem.*, **40**, 175 (1997).
26. S. M. Montemayor and A. F. Fuentes, *Ceram. Int.*, **30**, 393 (2004).
27. S.-J. Chen, X.-T. Chen, Z. Xue, J.-H. Zhou, J. Li, J.-M. Hong and X.-Z. You, *J. Mater. Chem.*, **13**, 1132 (2003).
28. O. Akhavan and E. Ghaderi, *Acs Nano*, **4**, 5731 (2010).
29. T. Amna, M. S. Hassan, D. R. Pandeya, M.-S. Khil and I. Hwang, *Appl. Microbiol. Biotechnol.*, **97**, 4523 (2013).
30. M. Oves, M. Arshad, M. S. Khan, A. S. Ahmed, A. Azam and I. M. Ismail, *J. Saudi Chem. Soc.*, **19**, 581 (2015).
31. M. Almeida, L. Cavalcante, J. A. Varela, M. S. Li and E. Longo, *Adv. Powder Technol.*, **23**, 124 (2012).
32. Y. Chang, S.-T. Yang, J.-H. Liu, E. Dong, Y. Wang, A. Cao, Y. Liu and H. Wang, *Toxicol. Lett.*, **200**, 201 (2011).
33. S. Chen, Y. Guo, S. Chen, H. Yu, Z. Ge, X. Zhang, P. Zhang and J. Tang, *J. Mater. Chem.*, **22**, 9092 (2012).
34. M. S. Hassan, T. Amna, D. R. Pandeya, A. Hamza, Y. Y. Bing, H.-C. Kim and M.-S. Khil, *Appl. Microbiol. Biotechnol.*, **95**, 213 (2012).
35. P. K. Stoimenov, R. L. Klinger, G. L. Marchin and K. J. Klabunde, *Langmuir*, **18**, 6679 (2002).